Optimization of taxane binding to microtubules. Binding affinity dissection and incremental construction of a high-affinity analogue of paclitaxel.

Ruth Matesanz[a*], Isabel Barasoain[a*], Chun-Gang Yang[b,c], Lei Wang[b,e], Xuan Li[b], Concepción de Inés[a], Claire Coderch[d], Federico Gago[d], Jesús Jiménez Barbero[a], José Manuel Andreu[a], Wei-Shuo Fang[b,c,f] and José Fernando Díaz[a,f,g].

[a]Centro de Investigaciones Biológicas, Consejo Superior de Investigaciones Científicas, Ramiro de Maeztu 9, 28040 Madrid, Spain

[b]Institute of Materia Medica, Chinese Academy of Medical Sciences, 1 Xian Nong Tan Street, Beijing 100050, P. R. China.

[c]Key Laboratory of Bioactive Substances and Resources Utilization of Chinese Herbal Medicine, Peking Union Medical College (Ministry of Education), Beijing 100050, P. R. China

[d]Department of Pharmacology, University of Alcalá, 28871 Alcalá de Henares, Spain.

[e]Present address: College of Life Sciences, Jilin University, Changchun, Jilin 130012, P. R. China.

[f]Corresponding authors.

[g]Contact address: fer@cib.csic.es Telephone: +34-918373112 ext 4269, Fax:+34-915360432.

[*]These authors have contributed equally to this work

Running title: Thermodynamics-driven design of novel taxanes.

This paper is dedicated to the memory of our late colleague Dr. Ángel R. Ortíz.

Summary

The microtubule binding affinities of a series of synthetic taxanes have been measured with the aims of dissecting individual group contributions and obtaining a rationale for the design of novel compounds with the ability to overcome drug resistance. As previously observed for epothilones, the positive and negative contributions of the different substituents to the binding free energies are cumulative. By combining the most favourable substitutions we increased the binding affinity of paclitaxel 500-fold. Insight into the structural basis for this improvement was gained with molecular modelling and NMR data obtained for microtubule-bound docetaxel. Taxanes with affinities for microtubules well above their affinities for P-glycoprotein are shown not to be affected by multidrug resistance. This finding strongly indicates that optimization of the ligand-target interaction is a good strategy to overcome multidrug resistance mediated by efflux pumps.

Introduction

Cancer is one of the major causes of premature death in humans and multidrug resistance (MDR) of neoplastic tissues is a major obstacle in cancer chemotherapy. While many tumours initially respond favourably to chemotherapeutic treatment, effectiveness at tumour regression is limited by the development of resistance. Although several primary reasons account for the MDR, the predominant cause is the overexpression and drug efflux activity of several transmembrane proteins, as best exemplified by P-glycoprotein (P-gp) (Shabbits et al. 2001).

P-gp is a member of the ATP binding cassette (ABC) family, with broad substrate specificity for substances including anticancer drugs, peptides, and HIV protease inhibitors. It has been shown that the extent of drug resistance in human tumours correlates well with P-gp expression (Tan et al. 2000).

In a previous work with a small group of C-2 substituted cephalomannines (CPHs) (Yang et al. 2007) we noticed that the resistance indexes for high-affinity taxanes in MDR cells are much lower than those for the medium-affinity taxanes, paclitaxel (TXL) and docetaxel (DXL), used in clinical practice. These results suggested that increasing the binding affinity of these compounds might be an alternative to overcome MDR, the rationale for this being that affinity for tubulin is the main force driving the entrance of the ligand into cells.

When MDR cells are exposed to taxanes, two opposite forces control ligand uptake: on the one hand, binding to P-gp, which will pump the ligand out of the cell, and on the other hand, binding to tubulin, which will reduce the intracellular concentration of the ligand and will keep it bound inside the cell. Thus, the higher the binding affinity of the ligand for tubulin, the lower the intracellular concentration of free ligand. Since efflux relies on drug binding to P-gp, which in turn depends on free

ligand concentration, at intracellular ligand concentrations far below its dissociation constant from P-gp, the efflux will be strongly decreased. In the most extreme case of a ligand that binds covalently to the taxane site, such as the natural product cyclostreptin, every molecule entering the cell will be finally trapped by tubulin and the tumour cell's MDR phenotype will be completely circumvented (Buey et al. 2007).

Although numerous chemical and biological qualitative studies of the structure-activity relationships of taxanes have been performed ((Zefirova et al. 2005), (Kingston et al. 2007), an in-depth study of the contributions of the different substituents to the binding thermodynamics has not been performed. We have previously shown that for epothilone (EPO) derivatives (Buey et al. 2004) the thermodynamic contributions of the substituents are accumulative, that is, the same substitution on different ligands produces a similar change on the binding affinity. The effect of a single modification can thus be quantified, and both favourable and unfavourable contributions can be combined to build tailor-made ligands with the desired affinities.

We now report on the thermodynamics of binding of a set of 44 taxanes (called Chitax (CTX)), plus the three reference compounds, TXL, DXL and CPH (Figure 1), to cross-linked stabilized microtubules (MT) in order to quantify the contributions of single modifications at four specific locations of the taxane scaffold: two of them, C2, in the southern part of the molecule, and C13, where side chains have been described as essential for taxane activity (Chen et al. 1993b), and another two, C7 and C10, in the northern part of the molecule, where substituents have been shown as non-essential for taxane activity (Chen et al. 1993a)). It is known that the side chains at these positions accept modifications that modulate the activity, both favourably and unfavourably (Ojima et al. 1997), (Kingston et al. 1998), (Yang et al.

2007). The activity of these taxanes was investigated against the parental (A2780) and MDR P-gp–overexpressing (A2780AD) human ovarian carcinoma cell lines (Rogan et al. 1984). We were able to correlate the binding affinity of these tubulin ligands to their cytotoxicity in the resistant cells. Moreover, the resulting thermodynamic data was used to design novel high-affinity taxanes with the ability to overcome P-gp–related resistance. The higher affinity of these newly designed compounds has been rationalized by experimentally determining the tubulin bound conformation of DXL and by modelling the complexes of DXL, TXL and the best of the designed taxanes within the binding site of β-tubulin.

Results

Thermodynamics of binding of TXL analogues to stabilized MTs.

All the compounds were first shown to be TXL-like MT-stabilizing agents (MSA) (Supplemental Table I). Then, their affinity for the taxane-binding site was measured using the competition method previously employed (Buey et al. 2004) (Table I and Supplemental Table II). Every compound was initially measured using Flutax-2 as the competitor. Compounds 4, 11, 12, 13, 14, 19, 20 and 21 displayed very high affinities, completely displacing Flutax-2 at equimolar concentrations (Figure 2A). This indicated that they were in the limit of the range of measurement allowed by the previously employed test (Díaz et al. 2007).

To measure the binding affinity of these compounds more precisely, we used a direct competition experiment with a higher-affinity compound, EPO-B, whose binding affinity (7.5×10^8 M^{-1} at 35 ºC) has been previously determined (Buey et al. 2005) (Figure 2B). This allowed the precise determination of the binding affinities of compounds 4, 11, 12, 13, 14, 19, 20 and 21, whose values range between 1.42×10^8

M^{-1} for the compound with the lowest affinity, CTX-21, and $1.51x10^9$ M^{-1} for the highest-affinity compound, CTX-12. This method was validated when the binding affinities of compounds 11, 13, 19 and 21 (those in the range of 10^8 M^{-1}) were shown to be similar using either EPO-B or Flutax-2 (Supplemental Data) .

To confirm that the high affinity of compounds containing 3-N_3 Benzoyl at C2 does not originates from covalent binding of its reactive azido group to β-tubulin, we performed experiments in which the amounts of reversibly bound compounds 4, 12 and 14 were measured. The bound compounds could be extracted from the pellets and aqueous solutions with the aid of an organic solvent, indicating that they are not irreversibly bound.

Molecular Modelling

One conspicuous characteristic of the taxane-binding site in β-tubulin (Lowe et al. 2001) is the presence of the highly exposed side chain of His229 (located in the middle of helix 7 and positionally equivalent to Arg229 in α-tubulin) that splits the cavity into two major pockets. Because continuum electrostatic calculations predicted the imidazole ring of this residue to be doubly protonated at pH 6.5 (pK_{His229}=7.2), this ionization state was used in subsequent work.

Molecular dynamics (MD) studies of TXL, DXL and CTX-40 in aqueous solution provided us with a range of different conformers, the most abundant of which (Supplemental Figure S1) were independently studied in a first rigid-body approach by the automated docking program. Interestingly, the conformation previously reported for TXL (Lowe et al. 2001) (Snyder et al. 2001) using either DOCK or FlexX was also found by AutoDock amongst the best scoring solutions. Since similar poses were found for DXL (Supplemental Figure S2) and CTX-40 as well, this common

disposition of the taxane in the binding site of β-tubulin was used in the modelling of all the complexes. Noteworthy, these conformations are not the most populated in aqueous solution (data not shown) although they are sporadically observed in the course of transitions toward other more stable and “hydrophobically collapsed” conformations. The proposed docked conformation for TXL is then in fact coincident with that previously found in crystals of 7-mesylpaclitaxel, which was reportedly induced by specific interactions of the side chain at C13 with solvent (Gao et al. 1996).

The feasibility of the resulting modelled complexes was assessed by subjecting each of them to a 10-ns MD simulation followed by a simulated annealing procedure that provided us with a set of representative complex structures for further analysis and energy decomposition. In all cases, the ligand adopts a conformation in good agreement with the T-taxol geometry (Snyder et al. 2001) (Figure 3) and is anchored in the binding site through a common set of well-defined interactions. Thus, the oxetane oxygen of the taxane is engaged in a good hydrogen bond with the NH of Thr276 whereas another hydrogen bond is established between the amide or carbamate carbonyl oxygen on the C13 substituent and the Nε of His229. On the other hand, the common phenyl ring at C13 (3’-Ph) establishes very close van der Waals contacts with the hydrophobic side chains of Val23 and Ala233 whereas the benzoyl phenyl ring at C2 (2-OBz) gets lodged into another hydrophobic cavity, on the other side of His229, made up of the side chains of Leu217, Leu219, and Leu275. The offset stacking interaction of this latter phenyl with the imidazole ring of His229 (Supplemental Figure S3) is improved by the substituent at the meta position, whose 1,2- (methoxy, CTX-13) or 1,3-dipole (azide, CTX-40) additionally establishes a favourable electrostatic interaction with the amide dipole of the backbone peptide

bond between His229 and Leu230 (Figure 3). Of the three hydroxyl groups that are common to the four ligands studied, that present on the C13 substituent is consistently engaged in a hydrogen bonding interaction with the carboxylate of Asp26 in helix 1 and the backbone nitrogen of Arg369 whereas that at C7 can establish transient hydrogen bonds with the carboxamide group of Gln282. On the other hand, the hydroxyl at C1 is permanently exposed to the solvent.

The four complexes yielded very low RMS deviations for the protein atoms with respect to the refined β-tubulin–TXL structure 1JFF (~1.3 Å on average for 400 atoms). The major differences when compared to this particular complex are the presence of a different rotameric state for His229, which we propose is protonated at physiological pH, and improved stacking and hydrogen bonding interactions between the ligand and the protein as a consequence of the mutual adaptation brought about by the simulated annealing procedure.

NMR characterization of bound docetaxel

As a further step, and to provide an experimentally-based support for the modelling-derived conformations, which formed the basis for the quest of the structure-activity relationship, the MT-bound conformation of DXL was elucidated, under the experimental conditions used for determining the binding constants (supplementary file DXLNMR.pdb).

As previously shown, the transferred nuclear Overhauser enhancement (TR-NOESY) technique provides an adequate means to determine the bound conformation of ligands that exchange between free and bound states at a reasonably fast rate. TR-NOESY experiments were then performed on the DXL:MT sample at different mixing times. Negative crosspeaks were clearly observed at 310 K (Figure 4,

panels A and B), as expected for a ligand that binds to the assembled MTs preparation, in contrast with the lack of NOEs detected in the free state (Figure 4, panel C).

Two control experiments were performed employing either Flutax-2 instead of DXL (the effective k_{off} of Flutax-2 release from MTs is 1.63±0.18 s^{-1} (Diaz et al. 2000)) or both DXL and discodermolide (DDM) at equimolecular concentrations. No TR-NOESY signals were observed in the presence of Flutax-2, indicating that the effective k_{off} of DXL is higher than that previously measured for Flutax-2, and the DXL signals were cancelled out by DDM (whose affinity for the TXL-binding site is 100 times higher), indicating that DXL is effectively bound to the TXL site (Buey et al. 2005).

Cytotoxicity in resistant and nonresistant tumour cells.

To check the effects of the studied modifications on the cytotoxicities of the compounds and to validate the binding affinity approach as a tool to be used in ligand optimization we performed IC_{50} tests in A2780 human ovarian carcinoma cells and their MDR A2780AD counterparts (Table I, Figure 5A).

The cytotoxicities of the ligands in non-P-gp-overexpressing A2780 cells show a linear relationship (r = 0.81) with their binding affinities but only for those compounds with a ΔG at 35 ºC higher than –47.5 kJ mol^{-1} (K_b at 35 ºC higher than 10^8 M^{-1}), which points to a limit in the cytotoxicity that can be achieved. Thus, despite the increase in affinity of 3 orders of magnitude between CPH and CTX-40, the IC_{50} remained in the order of nanomolar.

In the case of the MDR A2780AD cells, a good linear relationship (r = 0.80) between cytotoxicities and binding affinities is observed for the full set of ligands,

strongly suggesting that for these P-gp–overexpressing cells tubulin binding is the main force competing with P-gp–mediated extrusion.

The best regression lines have slopes of 1.10 for A2780 cells and 0.61 for A2780AD cells, which indicates that P-gp–overexpression effectively reduces the intracellular drug concentration thus making it necessary to increase the load in order to exert a cytotoxic effect.

Intake of taxanes by tumour cells

The amount of compound made available for binding to the tubulin site was measured by employing radioactively labelled DXL and TXL, at the concentrations needed to stop the cell cycle in G_2/M, in two leukemic cell lines (U937 and K562) and the kidney epithelial non-tumour cell line PtK2 from *Potorus tridactylis*. In these conditions, the intracellular drug concentration, which ranges from 0.3 to 2.8 μM and represents a small percentage of the total drug and the cell tubulin concentrations (Supplemental Table III), increases with the total drug concentration and reaches a maximum in PtK2 cells at 300 nM DXL and 600 nM TXL. The equilibration of the ligand inside the cells is fast, with a half-life of 3 minutes for ^{14}C-DXL and 10 minutes for ^{3}H-TXL at a drug concentration of 1 μM. The drug inside the cell was found to be in the cytoplasm, with only a very small fraction bound to the nucleus, as expected.

Since the total intracellular drug concentration is more than one order of magnitude above its MT dissociation constant and much lower than the total tubulin concentration (which was considered to be ~5% of the total protein measured), the mass action law dictates that most of the compound inside the cells is essentially bound to tubulin and also that the intracellular concentration of free drug is close to the dissociation constant, i.e. 70 nM for TXL and 25 nM for DXL.

Discussion

The effects of modifications on the substituents attached to the baccatin scaffold on the cytotoxicity of taxanes have been qualitatively discussed in several reviews (Zefirova et al. 2005), (Kingston et al. 2007). However, the fact that these studies were performed in different cell lines precludes a rigorous evaluation of the relationship between structural changes and cytotoxicity. To quantify the effects of substitutions at a set of specific positions in a systematic way, the binding affinity for the taxane-binding site on β-tubulin has proved to be a more precise and objective parameter (Buey et al. 2004).

With all the binding constants determined at a given temperature (35 ºC), it has been possible to determine the changes in apparent binding free energy caused by single group modifications (Table II) and to select the most favourable substituents at the positions chosen for optimization. Once this knowledge was obtained, it became feasible to design several optimized taxanes, as demonstrated below.

(1) Effect on the binding affinity of changes at the C2 position.

C2 modifications have turned out to be the most effective in modulating the activity of taxanes. Thus, the 2-OBz is absolutely essential since either its removal (Chen et al. 1993b) or its replacement with other small side chains (Ojima et al. 1994), (Nicolaou et al. 1995) results in almost total loss of activity in the human colon cancer cell line tested. On the contrary, changes in the structure of the ring, including its replacement with non-aromatic or heterocyclic rings, result in only moderate losses of antitumour activity (Ojima et al. 1994). Introduction of substituents on the 2-OBz ring, (Nicolaou et al. 1994), (Kingston et al. 1998), (Yang et al. 2007) results in increases of activity for small groups at the *meta* position but loss of activity for the

other positions. Changes in the linker connecting the benzene ring to the taxane core also result in decreased biological activity (Wang et al. 2007).

Our results confirm and extend the qualitative data summarized above and provide a precise quantitative characterization of the effects of C2 modifications on binding affinity:

a) Changing the nature of the linker between the benzene ring and the taxane scaffold results in a large loss of binding free energy. Thus, the replacement of the ester by an ether, thioether or amine moiety (compounds 24, 25, 26, 27, 38 and 39) or by a thioester or an amide (compounds 22, 23, 42, 43 and 44) results in a heavy loss of binding free energy (up to 20 kJ mol^{-1}). This stringent requirement indicates that the angle between the benzyl ring and the taxane core has to be strictly preserved and must be related to steric hindrance, as previously discussed for the thiobenzoyl compounds 22 and 23 (Wang et al. 2007), because the analogues in which the benzyl group is replaced by an alkyl ester (compounds 2, 3, 9, 10 and 16) only display a moderate loss of binding free energy (5–6 kJ mol^{-1}), which can be assigned to the loss of interactions between the benzyl ring and the binding site.

b) Modification of the *meta* substituents on the benzyl ring leads to gains of binding free energy that are the largest for $–N_3$ (–11.2±1.1 kJ mol^{-1}) and $–OCH_3$ (–7.2 kJ mol^{-1}) substituents (compounds 4, 5, 11, 12, 13, 14, 20) and much smaller (–2-3 kJ mol^{-1}) for halogen atoms (compounds 6, 30 and 34) whereas other small groups (–CN and $–CH_3$) have no effect (compounds 7 and 8). On the other hand, other similarly small substitutions (–OH and $–CH_2OH$), (compounds 36 and 37), are detrimental, resulting in a loss of 7–9 kJ mol^{-1} of binding free energy.

c) Introduction of double substituents at the 2,4 (compounds 28, 29) and 2,5 (35) positions results in loss of binding affinity.

d) The thienoyl moiety (compounds 31 and 32) can effectively replace the benzoyl group.

Because previous work from our group (Buey et al. 2004), has shown that substitutions leading to gains in binding free energy also give rise to increased cytotoxicity, the $–N_3$ substituent at the meta position of 2-OBz was selected as the most suitable for molecule optimization.

(2) Effect on the binding affinity of changes at the C13 position.

The side chains present at position C13 in one semisynthetic (DXL) and two natural taxanes (CPH and TXL) were evaluated in order to choose the optimal one for binding. Although from the direct comparison of TXL and DXL alone (Diaz et al. 1993) it is not possible to assess the effect of the C13 side chain on the binding free energy due to the presence of additional differences in the substituents at C7 and C10, DXL showed a 1.9–fold larger binding affinity relative to TXL, which corresponds to a change of –1.6 kJ mol^{-1} in free energy of binding. A similar difference (2x) was observed in the cytotoxicity on 1A9 cells (Buey et al. 2005). On the other hand, the tubulin binding affinity and the cytotoxicity of CPH are about two times lower than those of DXL (Yang et al. 2007).

In our series, by comparing compounds TXL, DXL, CPH, 11, 12, 13, 14, 15, 17, 20, 21, 22, 23, 24, 25, 26, 27, 38, 39 and 40 differing only in the side chain at C13 present in the reference molecules, we can now establish that, of the three side chains, that of DXL provides the largest contribution to the binding free energy, ($\Delta\Delta G$ C13-DXL−C13-TXL=–3.2±0.9 kJ mol^{-1}, $\Delta\Delta G$ C13-CPH−C13-DXL= –5.6±1.1 kJ mol^{-1}).

(3) Effect on the binding affinity of the substituents present in the northern side of the taxane ring (C7 and C10).

Modifications on the northern face of TXL at positions C7 and C10 have little effect on tubulin binding, as expected from the previously described effects on cytotoxicity (Chen et al. 1993a). From all the substituents tested at C10, the best one turns out to be the propionyl group, which provides an incremental free energy change of around –0.5 kJmol^{-1} over the natural C10 acetyl. On the contrary, introduction of the same group at position C7 brings about a loss of 1.6 kJ mol^{-1} of binding free energy relative to the –OH present in TXL. For this reason, a propionyl at C10 and a hydroxyl at C7 were selected as optimal substituents at these positions.

Optimal taxane

According to the data measured, "the optimal taxane" should have DXL's side chain at C13, an *m*-N_3-benzoyl at C2, a propionyl at C10, and a hydroxyl at C7. Starting from compound 1, the first one in the series, with an apparent binding affinity of –39.4 kJ mol^{-1}, the resulting molecule should gain –5.6 kJ mol^{-1} from the replacement of the CPH side chain with that of DXL, –11.2 kJ mol^{-1} from the substitution of *m*-N_3-benzoyl for benzoyl at C2, –1.6 kJ mol^{-1} from the change of a propionyl at C7 to a hydroxyl, and –0.9 kJ mol^{-1} from the change of a hydroxyl at C10 to a propionyl. Taking all of these changes together, the optimal taxane would have a predicted ΔG at 35 ºC of –58.7 kJ mol^{-1}. When the compound was synthesized (CTX-40) and its binding affinity was measured using the EPO-B displacement method (K_b 35ºC=6.28±0.15x10^9 M^{-1}; ΔG = –57.7±0.1 kJ mol^{-1}), the experimental value was found to be in nice correspondence with the predicted value.

Structural interpretation of the binding data

Two different reasons have been proposed for the changes in activity due to modifications at C2, i) the need for a hydrophobic group to maintain the proper taxane conformation, or ii) direct interactions of the benzoyl with hydrophobic side chains of the protein (Zefirova et al. 2005). The modelling data support the view that the higher affinity of CTX-40 relative to TXL and DXL, which is mostly conferred by the phenylazide substituent present at C2, may largely stem from the simultaneous improvement of the stacking interactions with the imidazole ring of His229(+) and a better electrostatic interaction with Asp26 and Arg369 on the opposite side of the molecule resulting from a better anchoring of the ligand in the binding site. The same rationale applies to CTX-13, which has a methoxy substituent in place of the azide, and to a lesser extent for the derivatives containing halogen atoms. As regards the methyl, cyano, hydroxyl or hydroxymethyl substituents, they are likely to be found facing the solvent rather than orientated towards the binding pocket thus contributing negligibly to the binding affinity, in good accord with the experimental evidence.

Likewise, the enhanced affinity contribution of the DXL and CTX-40 side-chain at C13 relative to that of TXL arises from an improved hydrogen-bonding interaction of the carbamate NH relative to the amide NH with the carboxylate of Asp26.

Pre-release conformation of bound docetaxel.

Transferred NOESY signals arise from a free DXL molecule whose protons have been excited when still bound to the protein but have been relaxed after release from the binding site. Thus, the conformation deduced from these signals corresponds to a pre-release state of the ligand. It has been described that MT-

stabilizing agents binding to the TXL site reach their luminal final location through prior transient binding to a site located in the MT pore (Diaz et al. 2003), (Buey et al. 2007). Therefore the NMR structural data have to be interpreted with this caution.

Since DXT release from MT following excitation has to be fast in order to get trNOESY signals, the K_{off} of the ligand should be fast in the relaxation time scale. This is apparently in contradiction with the slow dissociation constant measured for TXL in a kinetic study, 0.091±0.006 s^{-1} (Diaz et al. 2003). Nonetheless this observed dissociation constant does not correspond to the release step but to the rate-limiting step of the reaction. The dissociation of taxanes from MT has been studied in detail using the fluorescent taxane derivatives Flutax-1 and Flutax-2, which dissociate from MT following a two-step mechanism (Diaz et al. 2000). The first step, which is the slower one (thus the one directly observed), has a kinetic rate constant of 0.022±0.001 s^{-1} (4-fold slower than that of TXL) while the second one (responsible for the release of the ligand to the medium and which can be measured only indirectly from the dependence of the kinetic rate constants on concentration) is nearly 100 times faster (k_{off}=1.63±0.18 s^{-1}).

In the absence of the fluorescent probe it is not possible to calculate the value of the kinetic rate constant of the release step of DXL dissociation (k_{off}). Control experiments with Flutax-2 performed in the same conditions did not show any trNOESY signal from this ligand, which indicates that its k_{off} value is not large enough to provide good trNOESY signals. Therefore, the effective kinetic rate of the release step of the dissociation process of DXL has to be higher. Since it is not unreasonable to think that the presence of the fluorescein moiety slows down the dissociation of Flutax-2 and the observed trNOESY crosspeaks for the DXL:MT ensemble are cancelled out by addition of DDM (a TXL-binding site ligand with a much higher

affinity (Buey et al. 2005)), it can be assumed that the detected signals arise from DXL in the last step of dissociation from MT which may be bound to either the external site or to a modified luminal site.

The basic features of the NMR-derived conformation might be extracted from the trNOESY crosspeaks. Clear NOEs are observed between the t-butyl protons and the 2-OBz protons (Figure 4B), while only extremely weak NOEs are observed between both aromatic (2-OBz and 3'-Ph) moieties (Figure 4D). The OAc-4 group also provides NOEs with both aromatic rings (Figure 4B). These experimental observations allow us to discard the presence of the so-called polar conformation for DXL when this molecule is bound to MT. The NMR-derived conformation is thus basically in agreement with the conformation derived from the modelling approach (see Supplemental Figure S4). Nevertheless, whilst the modelled structure is in agreement with the so-called T-taxol geometry (Snyder et al. 2001), the NMR-derived conformation is intermediate between this one and that dubbed collapsed-geometry (Vandervelde et al. 1993). In any case, the fact that both conformations are fairly similar and indeed resemble the T-taxol conformation possibly indicates that the prerelease step does not largely affect the conformation of DXL, and that the T-taxol conformation is stable in the protein environment. The only observed difference is probably due to the presence of His229, which in the modelled structure is found between the 2-OBz and the C13 side chain, thus further separating these two moieties. The NMR observations are in agreement with a closer proximity between the OBz and the tBu protons (ca. 4-5 Å) than that suggested by the modelled DXL–β-tubulin complex (ca. 5-6 Å). Under these constraints, the NMR-deduced prerelease bound geometry for DXL, which is close to that of T-taxol, is in agreement with that derived by the modelling procedure, and resembles that described for the tubulin-

bound conformation of TXL (Lowe et al. 2001) although the experimental conditions herein are markedly different.

Binding affinity, cytotoxicity and P-gp-overexpression-mediated multidrug resistance.

The double log plots representing cytotoxicity vs. tubulin binding affinity (Figure 5A) clearly indicate that, as in the case of EPOs and other taxane-binding site ligands, both magnitudes are related, with the binding affinity behaving as a good predictor of cytotoxicity. However, a deviation of the predicted behaviour can be noted from this data. There is an apparent cytotoxicity limit (IC_{50} = 1 nM) for these compounds against the non–P-gp–overexpressing cells. A review of the results from our earlier work (Buey et al. 2004), (Buey et al. 2005) indicates that there are no MSA with an IC_{50} below nM in these cells. Despite having binding constants of the order of 10^9 M^{-1}, DDM and several EPOs have IC_{50}´s in the order of 1 nM or higher. In fact, cis-CP-tmt-EPO-B (compound 19 in (Buey et al. 2004)), the compound with the highest affinity for the TXL-binding site so far described ($2.1x10^{10}$ M^{-1}) and also the most cytotoxic (IC_{50} = 0.1 nM), displays a binding affinity three orders of magnitude above that of TXL but only a 10-fold increase in cytotoxicity (Buey et al. 2004). These data suggest that a significant percentage of tubulin within the cell has to be bound to stop the cell cycle and thereby cytotoxicity is limited by the amount of compound that is needed to achieve this goal.

At the drug concentrations required to stop cell-cycle progression, the percentage of tubulin bound by the ligand is in the range of 2–20% of the whole available protein. In the drug intake experiments, the total amount of compound available at the concentrations needed to stop the cell cycle (or at the IC_{50}) is around one third (comparable) of the total amount of tubulin. Although this should be enough,

in principle, for binding to a significant percentage of the protein, the results indicate that the amount of ligand available for binding to the sites is effectively much smaller (2–10 %). The reason for this might be that while all the binding sites are inside the small volume occupied by the cells, the drugs have to pass through the cell membranes and reach a threshold intracellular concentration that is opposed by the detoxification pumps. If a significant percentage (say 2–5%) of cytoplasmic tubulin has to be bound for the taxane to exert its cytotoxicity and the amount of ligand available for protein binding is a small percentage (2-10%) of the total 1 nM concentrations, which is already a third of the total amount of tubulin in the cells, it comes out that for the MSA with a taxane way of action the 0.1–1 nM concentration is a limit for its cytotoxicity in cells. The same reasoning can be applied to a systemically distributed drug for which the minimal amount needed to kill the tumour cells is related to the amount of tubulin available for binding, which imposes a practical limit on the lowest dose that can be used.

However, if the goal is not to find a drug with the highest cytotoxicity possible (in fact, none of the newly synthesized high-affinity compounds has a remarkably better cytotoxicity on nonresistant cells than have TXL and DXL) but rather to find one with the ability to overcome the main problem appearing in patients undergoing treatment with MSA, namely P-gp–mediated resistance, attempts to increase the affinity would seem to be steps in the right direction. Cells overexpressing P-gp are in fact still sensitive to taxanes because they can still be killed by higher concentrations of either TXL or DXL. Nonetheless, since these concentrations are very high, normal non-tumour cells will also be affected and even differentially killed because of their inability to reduce the intracellular drug concentration instead of being differentially spared because of their lower division rate.

The data with A2780AD cells shows the expected correlation (although with a lower slope arising from their ability to reduce the intracellular drug concentration) between affinity and cytotoxicity that was previously observed for chemically related compounds (Buey et al. 2004) with no deviations being noted at the highest cytotoxicity values (9 nM for CTX-40). In this type of MDR cells the high-affinity drugs are nearly 100-fold more cytotoxic than the clinically employed taxanes (TXL and DXL) and display very low resistance indexes (as low as 1.3 for the highest affinity derivative, CTX-40). This result was confirmed with LoVo human colon carcinoma cells and their MDR LoVo-Dox counterparts (Grandi et al. 1986) (see Supplemental Data).

When the resistance indexes of the compounds are represented against their binding affinities (Figure 5B), a bell-shaped curve is observed: the resistance index shows a maximum for taxanes displaying similar affinities for tubulin and P-gp, and then rapidly decreases when the affinity of the compound for tubulin either increases or decreases. An exception to this rule is found for compounds having a halogen atom (or a methoxy group) at the *meta* position of 2-OBz (CTX-5, 6, 30, 34 and 35) as they exhibit a much lower resistance index than that of other compounds with equivalent affinity.

The results confirm our previous data with other high-affinity ligands or with covalent binders (which can be considered to have infinite affinity) whose cytotoxicity is unaffected by P-gp overexpression (e.g. DDM: IC_{50} values of 60 nM and 53 nM (I. Barasoain, unpublished data), or cyclostreptin: IC_{50} values of 43.5 nM and 51 nM (Buey et al. 2007) against A2780 and A2780AD cells, respectively), which is a clear indication that ligands with high affinity for the taxane-binding site can overcome the P-gp–mediated MDR phenotype. The rationale for this finding is that, in these cells,

the intracellular free concentration of the high-affinity binding drugs will be very low (see Supplemental Data (Figures S5, S6 and S7) for a detailed mathematical model). It is obvious that for the ligand to be pumped out it first has to bind to P-gp, and assuming that the kinetics of drug efflux follows a Michaelis-Menten behaviour, the ligand outflow will decrease with lower free ligand concentration. Since these ligands are tightly bound to tubulin, their intracellular free concentrations are of the order of their dissociation constants, which in the case of the high-affinity compounds (K_d of CTX-40 = 0.16 nM at 35ºC) are far below their dissociation constants from P-gp (which range between 35 nM for TXL and 88 nM for CTX-7) (Yang et al. 2007). This implies that, at concentrations able to exert cytotoxicity, the efficacy of P-gp to pump out the high-affinity compounds will be reduced by a factor between 200 and 1000 (see Supplemental Data). From the chemical point of view, this means that P-gp overexpression is irrelevant.

On the other hand, the low-affinity tubulin-binding ligands may escape the effect of the pump through a different mechanism. Since they need to reach concentrations that are much higher than those of either tubulin or P-gp to bind their target and thereby exert their cytotoxicity, the pump gets overloaded (saturated) and cannot effectively reduce the intracellular drug concentration. For this reason these ligands act as MDR reversal agents by themselves (Brooks et al. 2003).

The present results support the view (Buey et al. 2005, Buey et al. 2004) that binding affinity is the main variable to be maximized in attempts to increase the cytotoxicity of this type of compounds (although on nonresistant cells a practical limit is observed at around 1 nM concentration). Additionally, the high-affinity compounds can escape MDR due to P-gp overexpression by lowering the concentration of free ligand that can be pumped out by P-gp.

Significance.

The binding affinities of a series of synthetic taxanes for MTs have been measured with the aims of dissecting individual group contributions and obtaining a rationale for the design of novel compounds with the ability to overcome drug resistance. As previously observed for EPOs, the positive and negative contributions of the different substituents to the binding free energy are cumulative. By combining the most favourable substitutions in one single analogue the binding affinity was increased 500-fold over that of TXL. Insight into the structural basis for this improvement was gained when models were built that assigned an important role to the interactions of C2 and C13 substituents with the protonated side chain of His229. The relative orientation of these groups was found to be in agreement with NMR data obtained for MT-bound DXL.

The cytotoxicities of the compounds in ovarian carcinoma A2780 cells were found to correlate with their affinities, with an apparent cytotoxicity limit in the nanomolar range. A bell-shaped curve was obtained when the taxane resistance index was plotted versus the binding affinity showing that the P-gp–overexpressing multidrug resistant A2780AD cells are sensitive to the highest and lowest affinity compounds, whereas resistance indexes in the range of 100 to 1000 were obtained for those whose binding affinities for tubulin and P-gp are similar.

The finding that taxanes with affinities for MTs well above their affinities for P-gp are not affected by multidrug resistance strongly indicates that for a series of compounds with similar pharmacokinetic and bioavailability properties, optimization of the ligand-target interaction is a good strategy to overcome multidrug resistance mediated by efflux pumps.

Experimental procedures.

Proteins and ligands.

Purified calf brain tubulin and chemicals were as described (Diaz et al. 1993). Full details of the synthesis and characterization of the ligands employed can be found as Supplemental Data.

Ligand-induced tubulin assembly.

Critical concentrations of ligand-induced tubulin assembly were measured as described (Buey et al. 2005).

Equilibrium binding constants of the ligands to MTs and tubulin.

The binding constants of the ligands with apparent binding affinities below 10^8 M^{-1} for the TXL-binding site were measured as described (Buey et al. 2004). For the EPO-B method, samples of 1 mL containing 1 μM sites in glutaraldehyde-stabilized MTs, 1.1 μM EPO-B and 1.1 μM of the test compound in GAB (glycerol assembly buffer; 3.4 M glycerol, 10 mM sodium phosphate, 6 mM $MgCl_2$, and 1 mM EGTA, pH 6.7) with 0.1 mM GTP were incubated for 30 minutes at 35 ºC in polycarbonate centrifuge tubes (Beckman). The samples were then centrifuged at 90,000 x g for 20 minutes at 35 ºC in a TLA-100.2 rotor employing a Beckman Optima TLX ultracentrifuge. The supernatants were collected by pipetting, and the pellets were resuspended in 10 mM phosphate buffer pH 7.0. 1 μM TXL was added as the internal standard, except for the experiments with CTX-13 in which 1 μM DXL was used instead. Both the pellets and the supernatants were extracted three times with an excess volume of dichloromethane, dried in vacuum and dissolved in 35 μl of methanol. The samples were analyzed by HPLC as described below

Reversibility of binding was checked by incubating samples containing 5 μM compounds 4, 12 or 14 and 10 μM taxoid binding sites in stabilized crosslinked MT, for 30 min at 25ºC in polycarbonate centrifuge tubes (Beckman) in GAB with 0.1 mM GTP (DMSO concentration was always kept under 2%). The samples were then centrifuged at 90000 g for 10 min at 25ºC in a Beckman Optima TLX ultracentrifuge with a TLA100 rotor, processed and analyzed as described above.

Binding constants for compounds reversibly displacing Flutax-2 or EPO-B were calculated using Equigra v5 (Díaz et al. 2007). The thermodynamic parameters (apparent ΔG_0, ΔH_0 and ΔS_0) were calculated as described (Buey et al. 2005).

Binding of the compounds to unassembled dimeric tubulin was measured by centrifugation. 200 μL samples containing 20 μM tubulin and 25 μM compound in 10 mM phosphate 1 mM EDTA, pH 7.0 buffer (PEDTA) containing 1 mM GDP were incubated for 1 h at 35 ºC in polycarbonate centrifuge tubes (Beckman). The samples were then centrifuged at 386,000 x g for 1 h at 35 ºC in a TLA100 rotor employing a Beckman Optima TLX ultracentrifuge. The upper and lower 100 μL of the solution were carefully collected by pipetting, and the pellets were resuspended in 10 mM phosphate buffer pH 7.0. The tubulin concentrations in the three samples were measured by the Bradford assay, and 5 μM DXL was added as the internal standard. The samples were extracted and analyzed as described above.

HPLC analysis of all samples was performed in an Agilent 1100 series instrument employing a Supercosil, LC18 DB, 250x4.6 mm, 5 mm bead diameter column developed in a gradient from 50–80% (v/v) acetonitrile in water at a flow rate of 1 mL min^{-1}, following the absorbance at λ=220 nm.

Cell biology studies.

PtK2 (kidney epitelial cell from *Potorus tridactylis*), U937 (monocytic human leukemia), K562 (myelocytic human leukemia), A2780, P-gp–overexpressing A2780AD (ovarian carcinoma) cells were cultured as previously described (Buey et al. 2005). Cytotoxicity assays were performed with the MTT assay modified as described in (Yang et al. 2007).

Cell intake of ^{3}H-TXL and ^{14}C-DXL were measured as reported (Manfredi et al. 1982) with modifications, using PtK2, U937, K562 cells. These cells, and especially the PtK2 cells, were used because they are more resistant to taxanes and more reproducible results could be obtained. Cells were grown in 24-well plates at a density of 500,000 cells/mL (PtK2) or 300,000 cells/mL (leukemic cell lines) and were incubated in 1 mL of medium with the desired drug concentration. Supernatants were collected and cells were washed 3 times with 1 mL of cold PBS and incubated overnight with 0.25 mL of NaOH 0.1M, and then neutralized with 0.25 mL of HCl 0.1 M. The total protein concentration was determined by the Lowry method and the drug (both in the supernatants and incorporated into cells) was measured by liquid scintillation counting in a LKB 1219 spectrometer. The correction for unspecific binding was determined by measuring the amount incorporated in cells preincubated with 10 μM colchicine for 4 h at 37ºC and washed three times prior to the incubation with ^{3}H-TXL or ^{14}C-DXL. Cell volume was calculated from the volume occupied by the pellets and was found to be 2.5±0.2, 3.96±0.05 and 4.3±0.9 μL/10^{6} cells for U937, K562 and PtK2, respectively.

The amounts of drugs bound to the nucleus and cytoplasm of the cells were determined as described in (Simpson et al. 1987).

Molecular Modelling

The refined structure of the α,β-tubulin dimer at 3.5 Å resolution (Lowe et al. 2001) (Protein Data Bank code 1JFF) was used for molecular modelling and ligand docking. Addition of missing hydrogen atoms and computation of the protonation state of ionizable groups in β-tubulin at pH 6.5 were carried out using the H++ Web server (Gordon et al. 2005), which relies on AMBER (Cornell et al. 1995) force-field parameters and finite difference solutions to the Poisson–Boltzmann equation. The molecular graphics program PyMOL (DeLano Scientific LLC) was employed for molecular visualization and representation. The charge distribution for the ligands studied was obtained by fitting the quantum mechanically calculated (RHF 6-31G*\\3-21G*) molecular electrostatic potential (MEP) to a point charge model, as implemented in Gaussian 03 (Gaussian, Inc., Wallingford CT, USA). Consistent bonded and nonbonded AMBER parameters were assigned to ligand atoms in the taxanes by analogy or through interpolation from those already present in the AMBER database (ff03).

The Lamarckian genetic algorithm implemented in AutoDock 3.0.5 (Morris et al. 1998) was used to generate automated docked poses of TXL, DXL, CTX-13, and CTX-40 within the taxane-binding site by randomly changing the overall orientation of conformers from the MD ensembles that were representative of the major populations, as well as the torsion angle involving the 2-OBz.

NMR experiments

The NMR experiments were performed at 310 K in D_2O as described (Jimenez-Barbero et al. 2006) with modifications described in supplementary data, on a Bruker AVANCE 500 spectrometer.

References

1. Brooks, T., Minderman, H., O'Loughlin, K.L., Pera, P., Ojima, I., Baer, M.R., and Bernacki, R.J. (2003). Taxane-based reversal agents modulate drug resistance mediated by P-glycoprotein, multidrug resistance protein, and breast cancer resistance protein. Mol Cancer Ther 2, 1195-1205.
2. Buey, R.M., Barasoain, I., Jackson, E., Meyer, A., Giannakakou, P., Paterson, I., Mooberry, S., Andreu, J.M., and Diaz, J.F. (2005). Microtubule interactions with chemically diverse stabilizing agents: Thermodynamics of binding to the paclitaxel site predicts cytotoxicity. Chem Biol 12, 1269-1279.
3. Buey, R.M., Calvo, E., Barasoain, I., Pineda, O., Edler, M.C., Matesanz, R., Cerezo, G., Vanderwal, C.D., Day, B.W., Sorensen, E.J., Lopez, J.A., Andreu, J.M., Hamel, E., and Diaz, J.F. (2007). Cyclostreptin binds covalently to microtubule pores and lumenal taxoid binding sites. Nat Chem Biol 3, 117-125.
4. Buey, R.M., Diaz, J.F., Andreu, J.M., O'Brate, A., Giannakakou, P., Nicolaou, K.C., Sasmal, P.K., Ritzen, A., and Namoto, K. (2004). Interaction of Epothilone Analogs with the Paclitaxel Binding Site; Relationship between Binding Affinity, Microtubule Stabilization, and Cytotoxicity. Chem Biol 11, 225-236.
5. Chen, S.H., Huang, S., Kant, J., Fairchild, C., Wei, J.M., and Farina, V. (1993a). Synthesis of 7-Deoxytaxol and 7,10-Dideoxytaxol Via Radical Intermediates. J Org Chem 58, 5028-5029.
6. Chen, S.H., Wei, J.M., and Farina, V. (1993b). Taxol Structure-Activity-Relationships - Synthesis and Biological Evaluation of 2-Deoxytaxol. Tetrahedron Lett. 34, 3205-3206.

7. Cornell, W.D., Cieplak, P., Bayly, C.I., Gould, I.R., Merz, K.M., Ferguson, D.M., Spellmeyer, D.C., Fox, T., Caldwell, J.W., and Kollman, P.A. (1995). A 2nd generation force-field for the simulation of proteins, nucleic-acids, and organic-molecules. J Am Chem Soc 117, 5179-5197.

8. Diaz, J.F., and Andreu, J.M. (1993). Assembly of purified GDP-tubulin into microtubules induced by taxol and taxotere: reversibility, ligand stoichiometry, and competition. Biochemistry 32, 2747-2755.

9. Diaz, J.F., Barasoain, I., and Andreu, J.M. (2003). Fast kinetics of Taxol binding to microtubules. Effects of solution variables and microtubule-associated proteins. J Biol Chem 278, 8407-8419.

10. Díaz, J.F., and Buey, R.M. (2007). Characterizing Ligand-Microtubule Binding by Competition Methods. In Methods in Molecular Medicine, Volume 137, J. Zhou, ed. (Totowa, NJ: Humana Press Inc.), pp. 245-260.

11. Diaz, J.F., Strobe, R., Engelborghs, Y., Souto, A.A., and Andreu, J.M. (2000). Molecular recognition of taxol by microtubules. Kinetics and thermodynamics of binding of fluorescent taxol derivatives to an exposed site. J Biol Chem 275, 26265-26276.

12. Gao, Q., and Chen, S.H. (1996). An unprecedented side chain conformation of paclitaxel (Taxol(R)): Crystal structure of 7-mesylpaclitaxel. Tetrahedron Lett. 37, 3425-3428.

13. Gordon, J.C., Myers, J.B., Folta, T., Shoja, V., Heath, L.S., and Onufriev, A. (2005). H++: a server for estimating pKas and adding missing hydrogens to macromolecules. Nucleic Acids Res 33, W368-371.

14. Grandi, M., Geroni, C., and Giuliani, F.C. (1986). Isolation and characterization of a human-colon adenocarcinoma cell-line resistant to doxorubicin. Brit J Cancer 54, 515-518.

15. Jimenez-Barbero, J., Canales, A., Northcote, P.T., Buey, R.M., Andreu, J.M., and Diaz, J.F. (2006). NMR determination of the bioactive conformation of peloruside a bound to microtubules. J Am Chem Soc 128, 8757-8765.

16. Kingston, D.G.I., Chaudhary, A.G., Chordia, M.D., Gharpure, M., Gunatilaka, A.A.L., Higgs, P.I., Rimoldi, J.M., Samala, L., Jagtap, P.G., Giannakakou, P., Jiang, Y.Q., Lin, C.M., Hamel, E., Long, B.H., Fairchild, C.R., and Johnston, K.A. (1998). Synthesis and biological evaluation of 2-acyl analogues of paclitaxel (Taxol). J Med Chem 41, 3715-3726.

17. Kingston, D.G.I., and Newman, D.J. (2007). Taxoids: Cancer-fighting compounds from nature. Curr. Opin. Drug Discov. Dev. 10, 130-144.

18. Lowe, J., Li, H., Downing, K.H., and Nogales, E. (2001). Refined structure of alpha beta-tubulin at 3.5 A resolution. J Mol Biol 313, 1045-1057.

19. Manfredi, J.J., Parness, J., and Horwitz, S.B. (1982). Taxol Binds to Cellular Microtubules. J Cell Biol 94, 688-696.

20. Morris, G.M., Goodsell, D.S., Halliday, R.S., Huey, R., Hart, W.E., Belew, R.K., and Olson, A.J. (1998). Automated docking using a Lamarckian genetic algorithm and an empirical binding free energy function. J. Comput. Chem. 19, 1639-1662.

21. Nicolaou, K.C., Couladouros, E.A., Nantermet, P.G., Renaud, J., Guy, R.K., and Wrasidlo, W. (1994). Synthesis of C-2 Taxol Analogs. Angew Chem Int Ed Engl 33, 1581-1583.

22. Nicolaou, K.C., Renaud, J., Nantermet, P.G., Couladouros, E.A., Guy, R.K., and Wrasidlo, W. (1995). Chemical Synthesis and Biological Evaluation of C-2 Taxoids. J Am Chem Soc 117, 2409-2420.

23. Ojima, I., Duclos, O., Zucco, M., Bissery, M.C., Combeau, C., Vrignaud, P., Riou, J.F., and Lavelle, F. (1994). Synthesis and Structure-Activity-Relationships of New Antitumor Taxoids - Effects of Cyclohexyl Substitution at the C-3' and/or C-2 of Taxotere (Docetaxel). J Med Chem 37, 2602-2608.

24. Ojima, I., Kuduk, S.D., Pera, P., Veith, J.M., and Bernacki, R.J. (1997). Synthesis and structure-activity relationships of nonaromatic taxoids: Effects of alkyl and alkenyl ester groups on cytotoxicity. J Med Chem 40, 279-285.

25. Rogan, A.M., Hamilton, T.C., Young, R.C., Klecker, R.W., and Ozols, R.F. (1984). Reversal of Adriamycin Resistance by Verapamil in Human Ovarian-Cancer. Science 224, 994-996.

26. Shabbits, J.A., Krishna, R., and Mayer, L.D. (2001). Molecular and pharmacological strategies to overcome multidrug resistance. Expert Rev Anticancer Ther 1, 585-594.

27. Simpson, R.U., Hsu, T., Begley, D.A., Mitchell, B.S., and Alizadeh, B.N. (1987). Transcriptional Regulation of the C-Myc Protooncogene by 1,25-Dihydroxyvitamin-D3 in Hl-60 Promyelocytic Leukemia-Cells. J Biol Chem 262, 4104-4108.

28. Snyder, J.P., Nettles, J.H., Cornett, B., Downing, K.H., and Nogales, E. (2001). The binding conformation of Taxol in β-tubulin: A model based on electron crystallographic density. Proc Natl Acad Sci U S A 98, 5312-5316.

29. Tan, B., Piwnica-Worms, D., and Ratner, L. (2000). Multidrug resistance transporters and modulation. Curr Opin Oncol 12, 450-458.

30. Vandervelde, D.G., Georg, G.I., Grunewald, G.L., Gunn, G.W., and Mitscher, L.A. (1993). Hydrophobic collapse of taxol and taxotere solution conformations in mixtures of water and organic-solvent. J Am Chem Soc 115, 11650-11651.

31. Wang, L., Alcaraz, A.A., Matesanz, R., Yang, C.G., Barasoain, I., Díaz, J.F., Li, Y.Z., Snyder, J.P., and Fang, W.S. (2007). Synthesys, biological evaluation, and tubulin binding poses of C-2a sulfur linked taxol analogues. Bioorg Med Chem Lett 17, 3191-3194.

32. Yang, C., Barasoain, I., Li, X., Matesanz, R., Liu, R., Sharom, F.J., Diaz, J.F., and Fang, W. (2007). Overcoming Tumor Drug Resistence Mediated by P-glycoprotein Overexpression with high affinity taxanes: A SAR study of C-2 Modified 7-Acyl-10-Deacetil Cephalomannines. Chem Med Chem 2, 691-701.

33. Zefirova, O.N., Nurieva, E.V., Ryzhov, A.N., Zyk, N.V., and Zefirov, N.S. (2005). Taxol: Synthesis, bioactive conformations, and structure-activity relationships in its analogs. Russ. J. Organ. Chem. 41, 315-351.

Acknowledgements

We wish to thank F. Amat-Guerri for Flutax-2, K.C. Nicolaou for EPO-B, the late M. Suffness for TXL, Rhône Poulenc Rorer Aventis for DXL and to José J. Ramírez and Tulsi Pindolia for their help in the early stages of the molecular modelling work. We also would like to thank Carne Sierra Madrid S.A. (CIF:A78074168) for providing the calf brains for tubulin purification. This work was supported in part by grant BIO2007-61336 from MEC to JFD, BIPPED-CM from Comunidad de Madrid to FG, JFD, JJB and JMA and grants NSFC No. 20572135 and MOST No.2006DFA31490 to WSF.

Figure Legends

Figure 1. Chemical structure of the taxanes employed in this study.

Figure 2. (A) Displacement of the fluorescent taxane Flutax-2 bound to MT sites (50 nM) by taxanes at 35 ºC. The solid lines were generated with the best fit value of the binding equilibrium constant of the competitors with binding affinities lower to 10^7 M^{-1}, assuming a one-to-one binding to the same site. Additional lines (dashed lines) show the expected displacement for ligands with binding constants of 10^8 M^{-1} (black), 10^9 M^{-1} (red), 10^{10} M^{-1} (green), and 10^{11} M^{-1} (yellow). Ligands binding data are as follows: green CPH, red CTX-2, yellow CTX-6, dark blue, CTX-11, magenta CTX-12, light blue CTX-14, black CTX-27. (B) Displacement of EPO-B bound to MT sites (10 μM) by CTX-40 at 35 ºC. 1 μM TXL-binding sites were incubated with 1.1 μM EPO-B (black lines) or with 1.1 μM EPO-B and 1.1 μM CTX-40 (red lines), MTs were harvested by sedimentation, ligands extracted from supernatants (solid lines) and pellets (dashed lines) and HPLC analyzed. 1 μM TXL is used as the internal standard. Supernatant traces were displaced 40 mAU for presentation purposes.

Figure 3.-TXL (A) and CTX-40 (B) in the binding site of β-tubulin at the end of the simulated annealing procedure. Note that the doubly protonated imidazole ring of His229 participates in (i) a hydrogen bonding interaction with the amide or carbamate carbonyl oxygen on the C13 substituent through the Nε, and (ii) an offset stacking interaction with the phenyl ring on the C2 substituent.

Figure 4. A.- The 500 MHz TR-NOESY (mixing 200 ms, 303 K) spectrum of DXL in buffered water solution in the presence of MTs (20:1 molar ratio). B.- Expansion showing the key TR-NOESY region: close contacts between the tert-butyl chain and the aromatic 2-OBz ring (besides the trivial cross peaks with the vicinal 3'-Ph moiety). C.- The NOESY experiment under the same experimental conditions (200 ms) in the

absence of MTs did not basically show any cross peak. D.- Expansion of the aromatic region in the TR-NOESY spectrum: Basically, no NOEs between the two aromatic 3'-Ph and 2-OBz moieties are observed.

Figure 5. (A) Dependence of the IC_{50} of the ligands against A2780 (black) and A2780AD (grey) human ovarian carcinoma cells on the affinity for the TXL-binding site in MTs (binding constant, K_b). The black line represents the best fit of IC_{50} against A2780 cells vs binding affinity for ligands with binding affinity under $5x10^8$ M^{-1}. The grey line represents the best fit of IC_{50} against A2780AD cells vs binding affinity. (B) Dependence of the resistance index of the A2780AD MDR cells on the affinity of the compounds for the taxane binding site. The range of binding affinities of taxanes for P-gp was taken from (Yang et al. 2007).

Tables.

Table I. Apparent binding affinities, thermodynamic parameters of binding of taxanes for the TXL site (10^7 M^{-1}) and cytotoxicity of the compounds to non-resistant and resistant ovarian carcinoma cells.

Compound	Kb 35ºC	ΔG 35ºC kJ/mol	ΔH kJ/mol	ΔS J/mol	IC_{50} A2780 nM	IC_{50} A2780AD nM	R/S
TXL[a]	1.43±0.17	-42.1±0.3	-51±4	-29±13	1.3±0.4	980±149	753
DXL[a]	3.93±0.27	-44.8±0.2	-53±2	-26±8	0.6±0.2	290±16	483
CPH	0.69±0.08	-40.3±0.3	-39±6	-6±18	1.5±0.2	910±285	606
CTX-1	0.49±0.12	-39.4±0.6	-56±12	-56±39	13.2±7	1222±300	92.5
CTX-2	0.043±0.018	-33.2±0.9	-66±18	-109±38	950±80	10200±1900	10.7
CTX-3	0.072±0.017	-34.5±0.5	-32±9	10±29	1250±200	4000±700	3.2
CTX 4[b]	87±19	-52.7±0.5	-46±13	19±44	2.7 ±0.6	14±3.8	5.2
CTX-5	5.37±1.39	-45.6±0.6	-40±4	19±14	6.6±1.8	160±19	24.2
CTX-6	1.62±0.24	-42.5±0.4	-39±2	13±7	10±2.4	274±30	27.4
CTX-7	0.39±0.06	-38.8±0.4	-38±5	4±17	14.5±2.9	2100±660	145
CTX-8	0.492±0.073	-39.4±0.3	-28±3	39±10	22.5±5	596±105	26.4
CTX-9	0.028±0.008	-32.1±0.6	-15±4	56±12	3900±370	15000±3500	3.8
CTX-10	0.042±0.008	-33.1±0.4	-12±5	68±18	4900±600	>20000	>4
CTX 11[b]	38±10	-50.5±0.6	-14±20	117±65	1.36±0.2	163±37	120
CTX 12[b]	151±3	-54.1±0.1	-29±9	84±29	2.8±0.38	42±13	15
CTX 13[b]	16.5±2.8	-48.4±0.4	-28±1	66±1	1.3±0.2	128±17	98.4
CTX 14[b]	80.0±2.9	-52.5±0.1	-46±6	21±19	1.6±0.3	25±10	15.6
CTX-15	2.384±0.53	-43.5±0.5	-18±11	80±35	17.5±2.7	5250±1000	300
CTX-16	0.050±0.030	-33.6±1.2	-18±9	49±30	740±100	7360±750	9.9
CTX-17	0.902±0.37	-41.0±0.9	-24±3	55±10	18±5.6	5412±1200	301
CTX-18	1.281±0.27	-41.9±0.5	-22±4	64±14	2.1±0.8	452±36	215.2
CTX 19[b]	14.8±0.2	-48.2±0.1	-48±3	0±9	0.54±0.07	39±11	72.2
CTX 20[b]	80.6±5.1	-52.5±0.2	-92±19	-124±64	3.9±1.2	27.4±4	7
CTX 21[b]	14.2±1.6	-48.0±0.3	-26±5	72±16	1.9±0.3	41±11	21.5
CTX-22	0.013±0.00	-30.1±0.0	-46±7	-151±23	2400±1000	6960±670	2.9
CTX-23	0.007±0.00	-28.6±0.0	-37±7	-123±22	11500±1000	23800±2200	2.1

CTX-24	0.094±0.01	-35.2±0.3	-65±10	-95±33	353±19	8600±3800	24.3
CTX-25	0.008±0.00	-28.9±0.0	-47±7	-154±24	6200±2600	28500±5300	4.6
CTX-26	0.018±0.00	-31.0±0.0	-73±11	-77±137	3500±1400	8300±2700	2.4
CTX-27	0.007±0.00	-28.6±0.0	-42±6	-138±21	10000±740	9400±1700	0.94
CTX-28	0.17±0.04	-36.7±0.5	-17±8	62±25	82±16	1880±200	22.9
CTX-29	0.25±0.08	-37.7±0.7	-52±9	-48±30	102±8.8	690±60	6.8
CTX-30	1.76±0.91	-42.7±1.1	-11±15	92±49	30±0.5	246±27	8.2
CTX-31	0.10±0.04	-35.4±0.9	-44±11	-30±36	106±4.2	2950±480	27.8
CTX-32	0.24±0.08	-37.6±0.7	-7±16	87±55	62±17	3200±250	51.6
CTX-33	0.07±0.01	-34.4±0.3	-81±12	-152±39	69±77	1500±100	21.7
CTX-34	1.20±0.93	-41.7±1.5	-38±28	14±94	28.7±1.9	196±14	6.8
CTX 35	0.88±0.77	-40.9±1.6	-29±33	13±112	25±2	153±39	6.12
CTX 36	0.029±0.020	-32.2±1.3	-48±6	-63±18	1700±120	>20000	>11.7
CTX 37	0.035±0.010	-32.7±0.6	-91±7	-207±24	86±9.8	10000±1000	116.2
CTX 38	0.001±0.001	-23.6±1.8	-44±9	-70±34	15400±3200	20000±3000	1.3
CTX 39	0.003±0.001	-26.4±0.7	-157±10	-461±28	4200±100	5700±300	1.3
CTX 40[b]	628±15	-57.7±0.1	-26±24	99±80	7±1	9.1±0.45	1.3
CTX 41	0.021±0.004	-31.4±0.4	-94±9	-202±28	14000±2000	>20000	1.4
CTX 42	0.008±0.003	-28.9±0.8	-106±13	-250±43	192±20	2750±430	14.3
CTX 43	0.030±0.008	-32.3±0.6	-85±20	-169±66	69.5±3.8	331±70	4.8
CTX 44	0.001±0.001	-23.6±1.8	-177±23	-493±75	>20000	>20000	

a) Binding affinity and thermodynamic parameters data are from (Buey et al. 2004).

b) Compounds measured with the EPO-B displacing method

Errors bars are standard errors of the mean

Table II. Incremental free energy of binding of TXL analogues to MTs due to single group modifications.

Modification type.	Modification	Compounds	ΔΔG	Avg (Std Err)
C2	Benzoyl → benzylether	T→25	+13.2	+13.0±0.2
		21→24	+12.8	
	Benzoyl → benzylsulphur	T→27	+13.6	+15.9±2.3
		21→26	+18.1	
	Benzoyl → benzylamine	T→38	+18.6	+20.1±1.5
		21→39	+21.6	
	Benzoyl → thiobenzoyl	T→23	+19.6	+15.9±3.8
		21→22	+12.1	
	Benzoyl → benzamide	21→42	+19.2	
	Benzamide → 3-OCH_3-benzamide	42→43	-3.4	
	Benzamide → 3-Cl-benzamide	42→44	+5.3	
	Benzoyl → 3-methyl- 2 butenoyl	1→2	+6.2	
	Benzoyl → 3-methyl- 3 butenoyl	1→3	+4.9	
	Benzoyl → 2(E)-butenoyl	1→9	+7.3	
	Benzoyl → 3-methyl- butanoyl	1→10	+6.3	
	Benzoyl → 2-debenzoyl-1,2-carbonate	C→16	+5.8	
	Benzoyl → 3-N_3 Benzoyl	1→4	-8.0	-11.2±1.3
		T→12	-13.9	
		C→14	-12.2	
		18→20	-10.6	
	Benzoyl → 3-OCH_3-benzoyl	1→5	-6.2	-7.2±0.6
		T→11	-8.3	
		C→13	-8.1	
		18→19	-6.3	
	Benzoyl → 3-Cl-benzoyl	1→6	-3.1	
	Benzoyl → 3-Br-benzoyl	1→34	-2.3	
	Benzoyl → 3-I-benzoyl	1→30	-3.3	
	Benzoyl → 3-NC-benzoyl	1→7	+0.6	
	Benzoyl → 3-CH3-benzoyl	1→8	0.0	
	Benzoyl → 3-CH_2OH-benzoyl	1→36	+7.2	
	Benzoyl → 3-OH-benzoyl	18→37	+9.2	
	3-Cl-Benzoyl → 2,4-di-Cl-benzoyl	6→29	+4.8	
	Benzoyl → 2,4-di-F-benzoyl	1→28	+2.7	
	3-OCH_3-Benzoyl → 2-5-di- OCH_3-benzoyl	5→35	+4.6	
	Benzoyl → 2-thienoyl	1→31	+4.1	
	Benzoyl → 3-thienoyl	1→32	+1.8	
	Benzoyl → 6-carboxy-pyran-2-one	1→41	+8.1	
C13 Side Chain	TXL → CPH	T→C	+1.9	+2.0±0.2
		11→13	+1.9	
		12→14	+1.6	

		15→17	+2.4	
	TXL → DXL	23→22	-1.7	-3.2±0.9
		25→24	-6.2	
		27→26	-1.3	
		38→39	-2.8	
		T→21	-4.2	
	CPH → DXL	C→21	-3.8	-5.6±1.1
		17→D	-7.7	
		20→40	-5.2	
C10	Acetyl → –OH	T→15	-1.3	-1.7±0.8
		C→17	-0.7	
		21→D	-3.2	
	Propionyl → –OH	18→17	+0.9	+0.9
	Acetyl → propionyl	C→18	-1.6	-0.5±0.4
		13→19	+0.2	
		14→20	0.0	
C7	Propionyl → –OH	17→1	-1.6	-1.6

Errors bars are standard errors of the mean

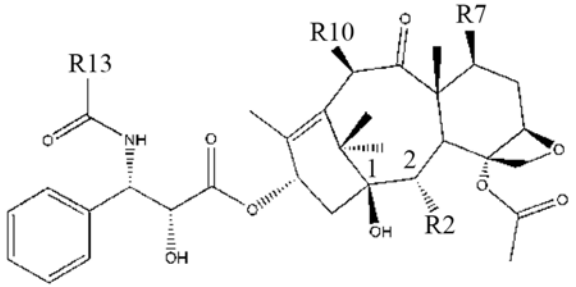

R13	R10	R7	R2	m	
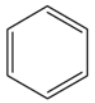		OH	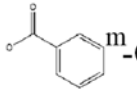	-H	**Paclitaxel**
				-OCH_3	**Chitax-11**
				$-N_3$	**Chitax-12**
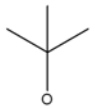	OH	OH	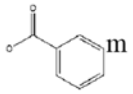	-H	**Docetaxel**
		OH	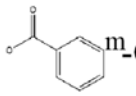	-H	**Cephalomannine**
				-OCH_3	**Chitax-13**
				$-N_3$	**Chitax-14**
	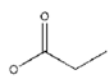	OH	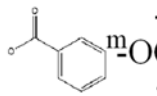	-H	**Chitax-18**
				-OCH_3	**Chitax-19**
				$-N_3$	**Chitax-20**
				-OH	**Chitax-37**

R13	R10	R7	R2	m	p	o	
	OH	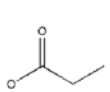	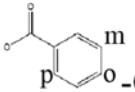	-H	-H	-H	**Chitax-1**
				$-N_3$	-H	-H	**Chitax-4**
				-OCH_3	-H	-H	**Chitax-5**
				-Cl	-H	-H	**Chitax-6**
				-CN	-H	-H	**Chitax-7**
				-CH_3	-H	-H	**Chitax-8**
				-H	-F	-F	**Chitax-28**
				-H	-Cl	-Cl	**Chitax-29**
				-I	-H	-H	**Chitax-30**
				-CHO	-H	-H	**Chitax-33**
				-Br	-H	-H	**Chitax-34**
				-OCH_3	-OCH_3	-H	**Chitax-35**
				-CH_2OH	-H	-H	**Chitax-36**

R13	R10	R7	R2		
	OH	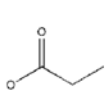	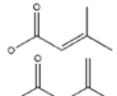		**Chitax-2**
					Chitax-3
			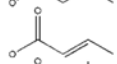		**Chitax-9**
			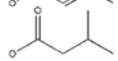		**Chitax-10**
		OH	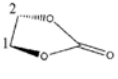		**Chitax-16**
	OH	OH	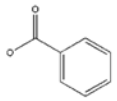		**Chitax-17**

R13	R10	R7	R2		
	OH	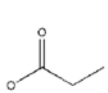	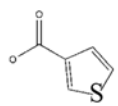		**Chitax-31**
			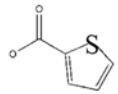		**Chitax-32**
			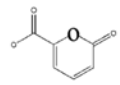		**Chitax-41**
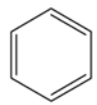	OH	OH	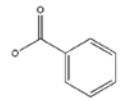		**Chitax-15**

R13	R10	R7	R2	m	
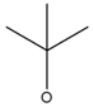	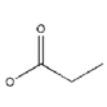	OH	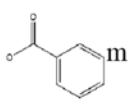	$-N_3$	**Chitax-40**

R13	R10	R7	R2	X	m	
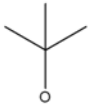	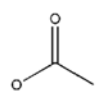	OH	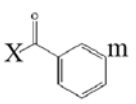	NH	-H	**Chitax-42**
				NH	-OCH_3	**Chitax-43**
				NH	-Cl	**Chitax-44**

R13	R10	R7	R2	X	a	
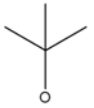		OH		O	=O	**Chitax-21**
				S	=O	**Chitax-22**
				O	$-H_2$	**Chitax-24**
				S	$-H_2$	**Chitax-26**
				NH	$-H_2$	**Chitax-39**
		OH		S	=O	**Chitax-23**
				O	$-H_2$	**Chitax-25**
				S	$-H_2$	**Chitax-27**
				NH	$-H_2$	**Chitax-38**

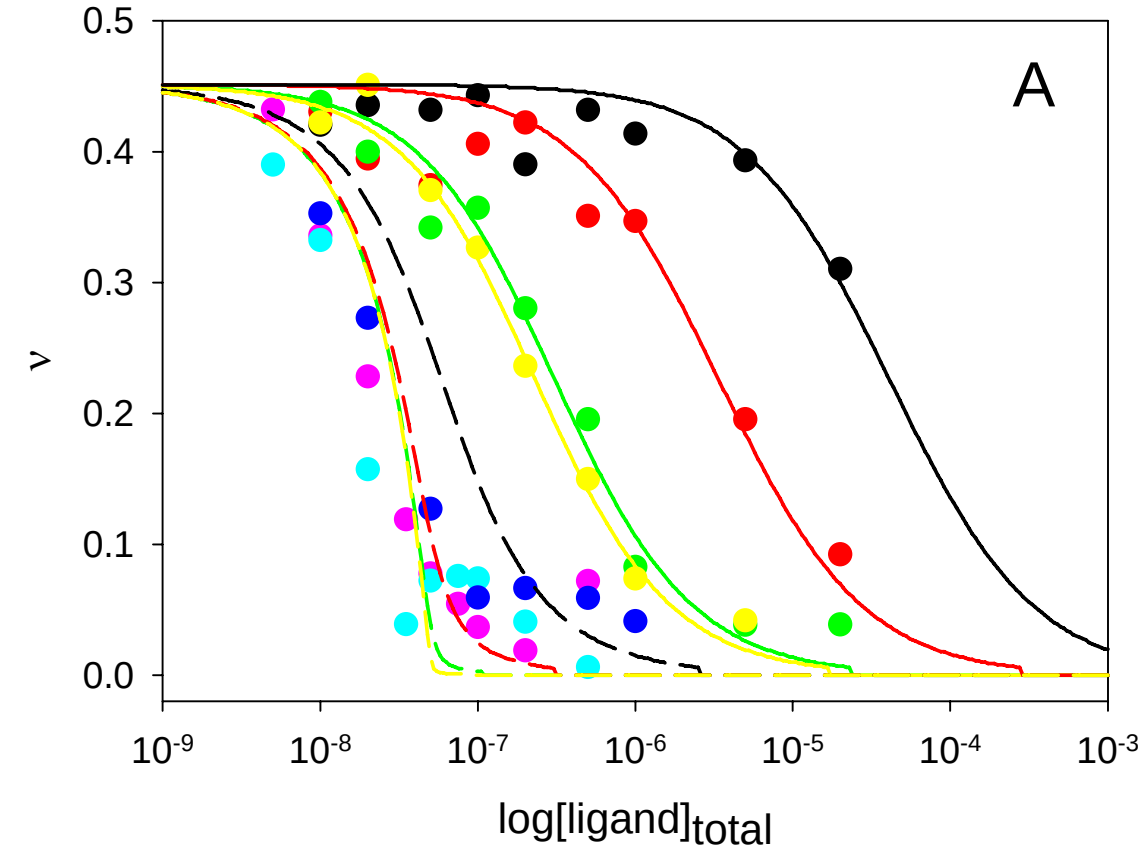
A
0.5
0.4
0.3
0.2
0.1
0.0
v
10-9
10-8
10-7
10-6
10-5
10-4
10-3
log[ligand]total

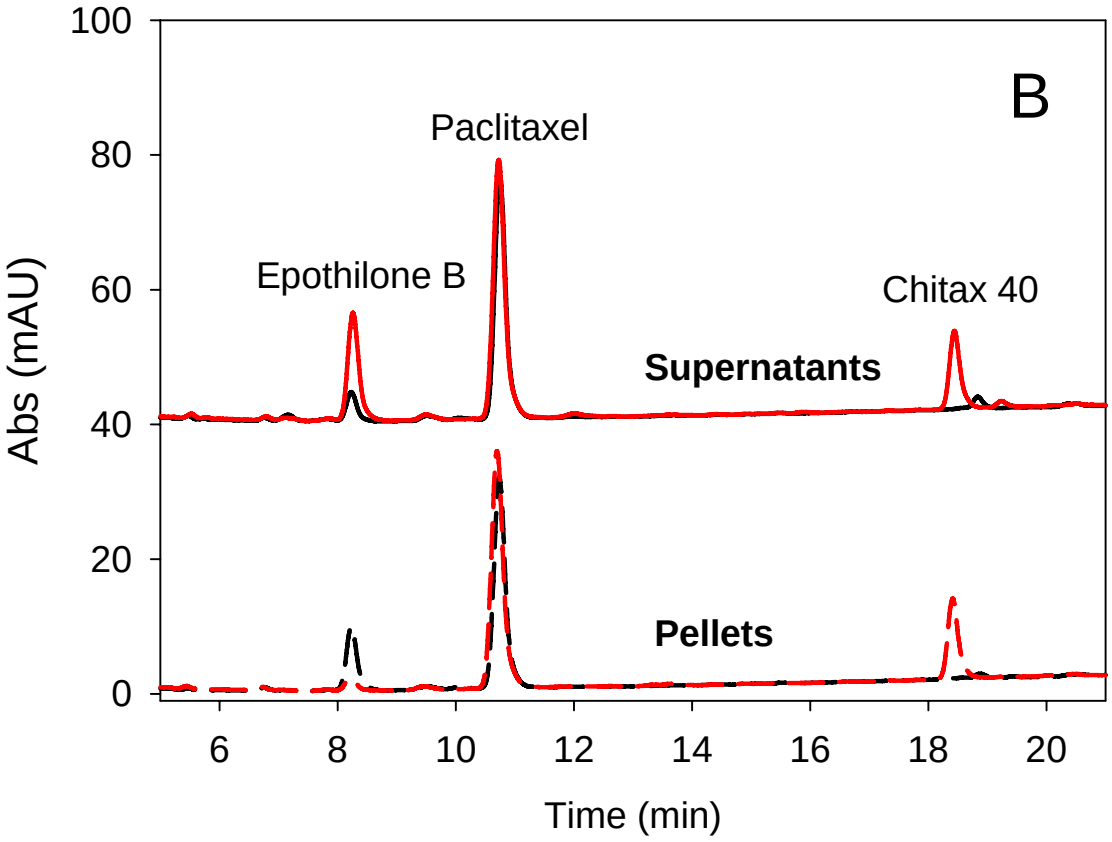
B
100
80
60
40
20
0
Abs (mAU)
Paclitaxel
Epothilone B
Chitax 40
Supernatants
Pellets
6
8
10
12
14
16
18
20
Time (min)

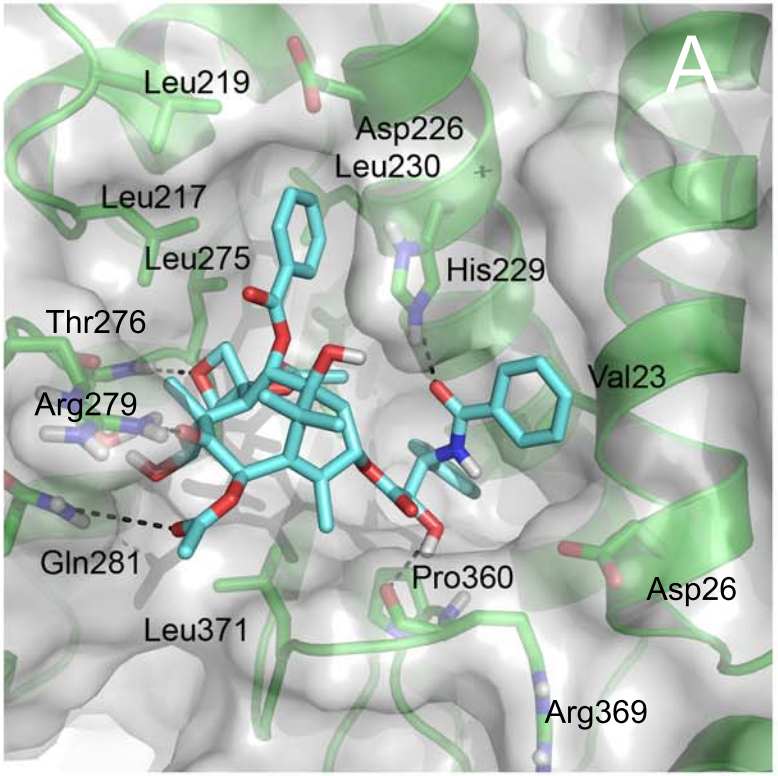
A
Leu219
Asp226
Leu230
Leu217
Leu275
His229
Thr276
Val23
Arg279
Gln281
Pro360
Asp26
Leu371
Arg369

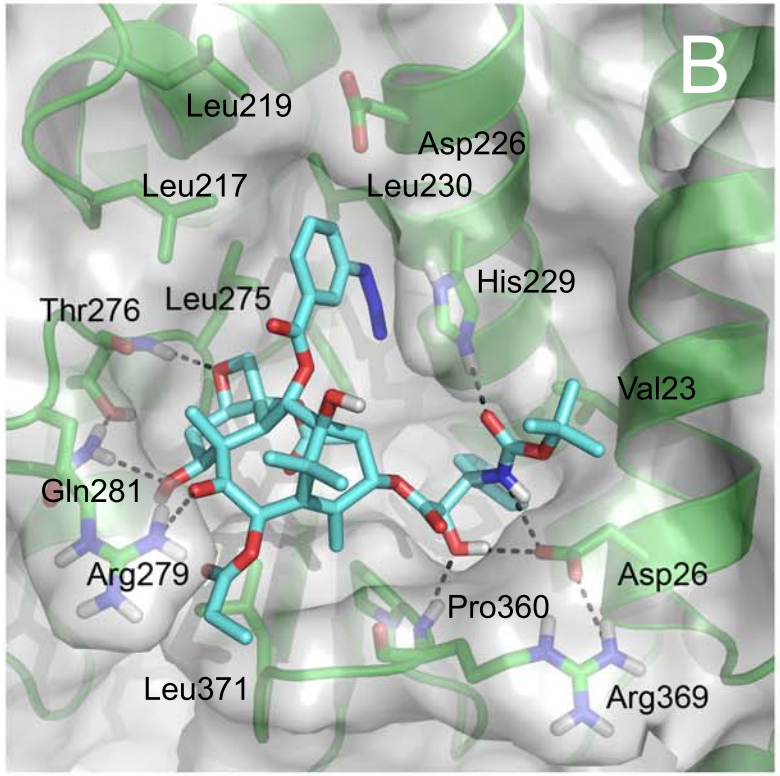
B
Leu219
Asp226
Leu217
Leu230
His229
Thr276
Leu275
Val23
Gln281
Arg279
Asp26
Pro360
Leu371
Arg369

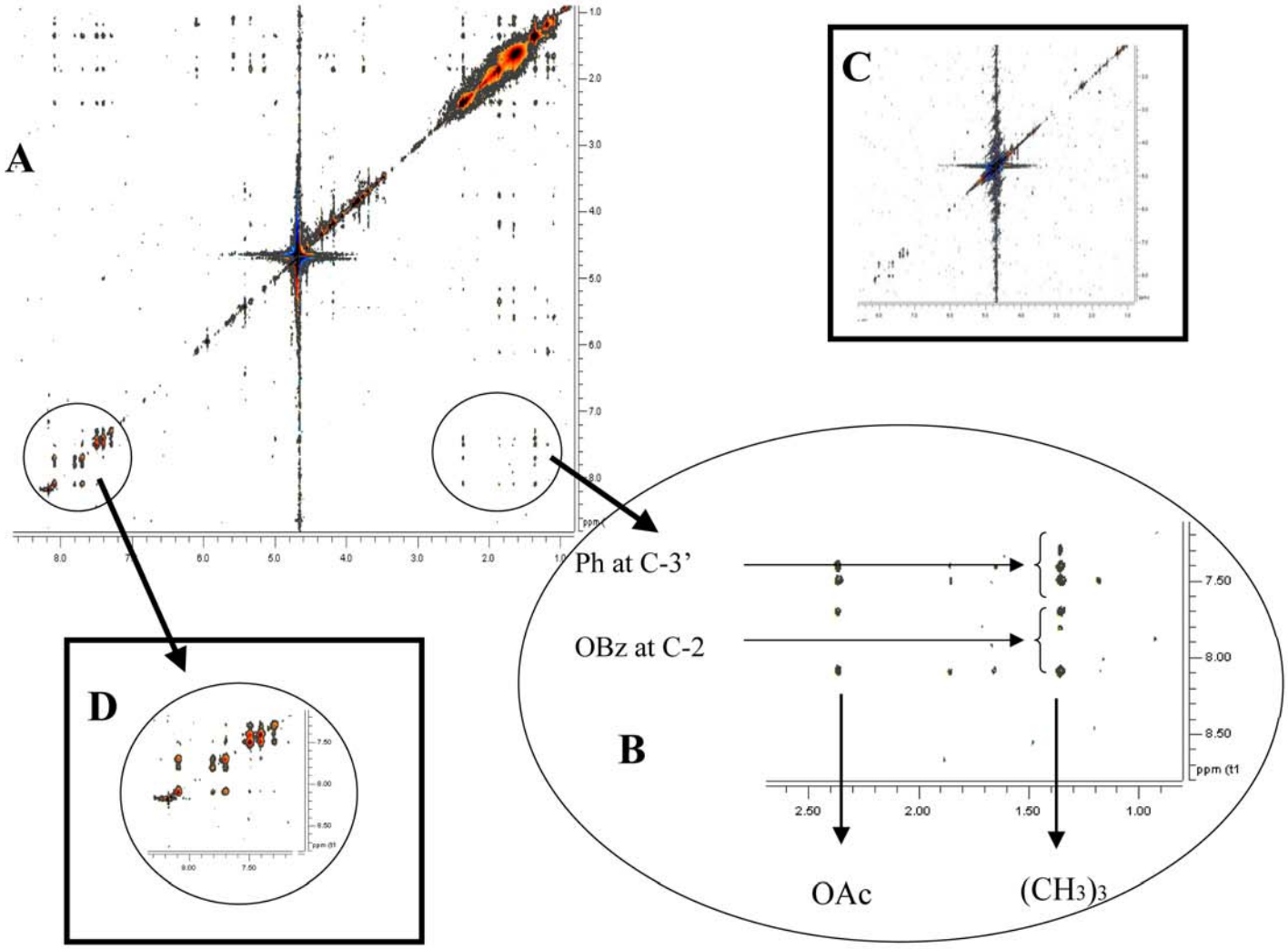
A
C
B
D
Ph at C-3'
OBz at C-2
OAc
(CH3)3
ppm (t1

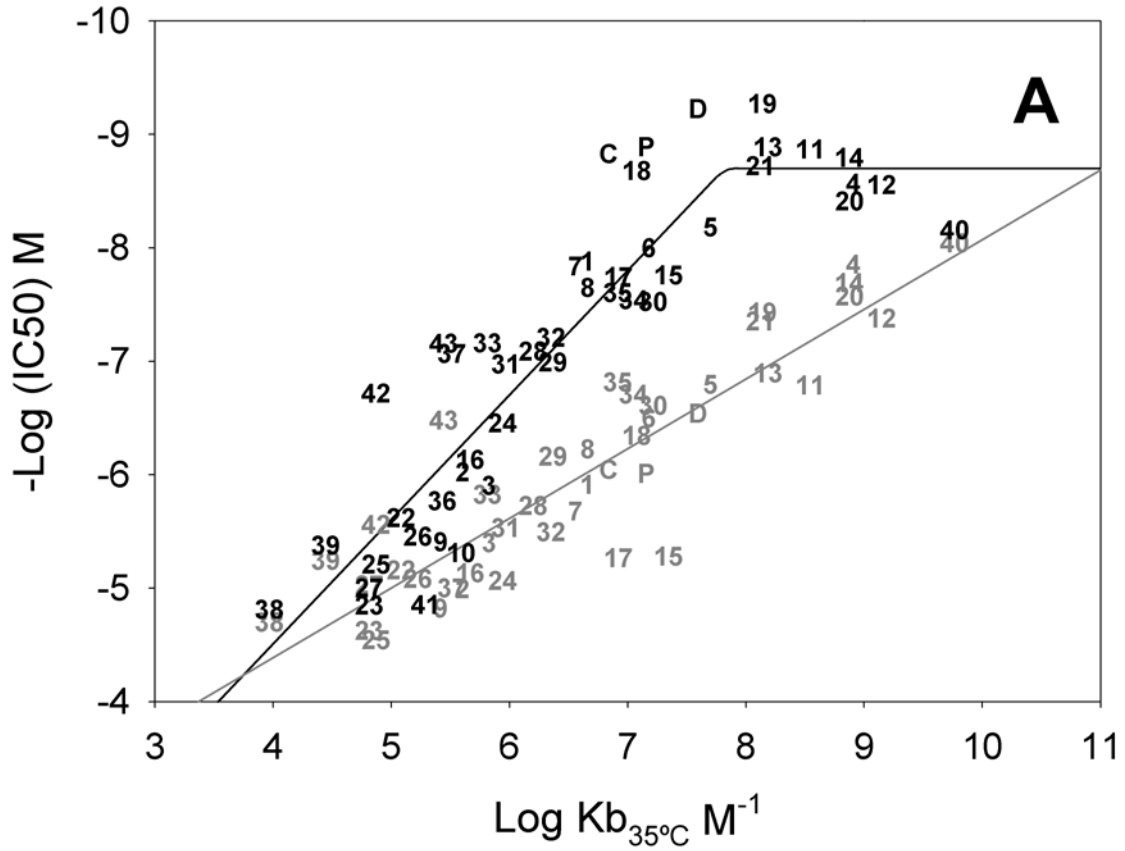
A
-Log (IC50) M
Log Kb35ºC M-1

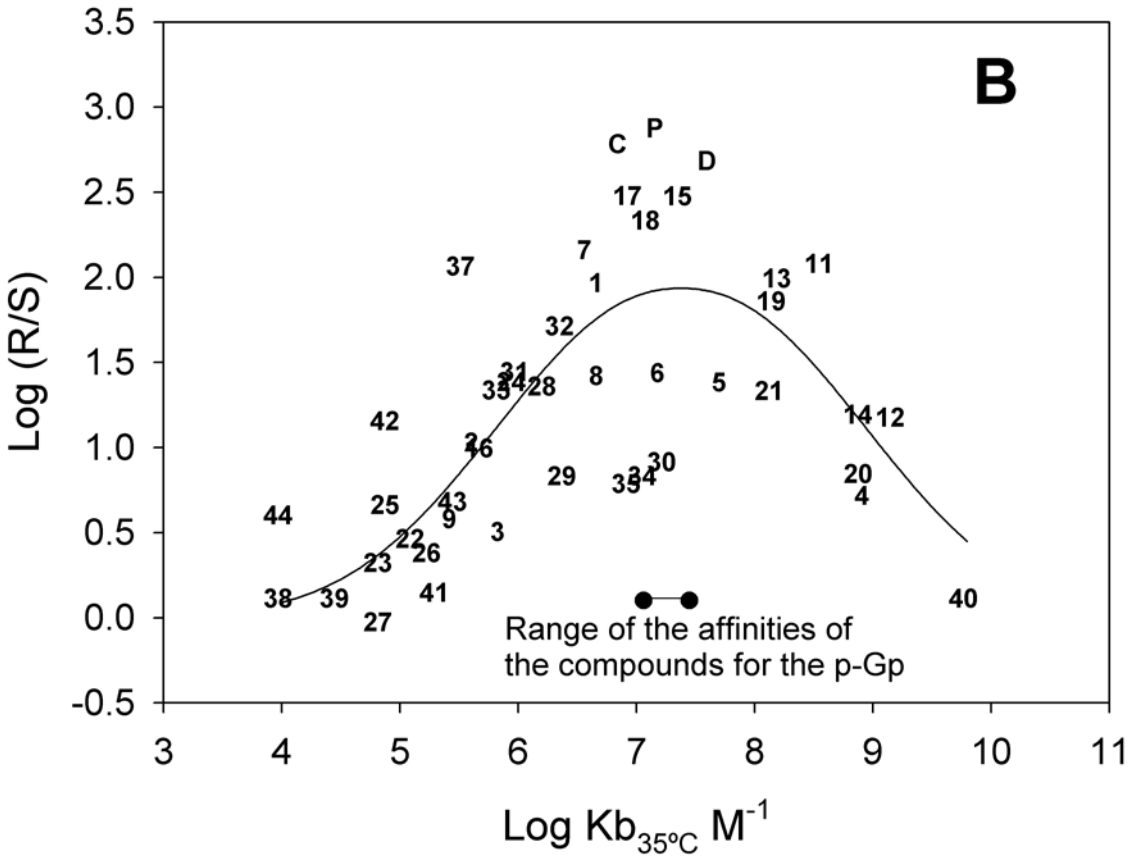
B
Log (R/S)
Range of the affinities of
the compounds for the p-Gp
Log Kb35ºC M-1